DT# 48004
QA: NA 5/31/06 CB

Modeling temporal-spatial earthquake and volcano clustering at Yucca Mountain, Nevada

Tom Parsons U. S. Geological Survey, Menlo Park, CA 94025

George A. Thompson Department of Geophysics, Stanford University, CA 94305

Allen H. Cogbill Los Alamos National Laboratory, Los Alamos, NM 87545

ABSTRACT

The proposed national high-level nuclear repository at Yucca Mountain is close to Quaternary faults and cinder cones. The frequency of these events is low, with indications of spatial and temporal clustering, making probabilistic assessments difficult. In an effort to identify the most likely intrusion sites, we based a 3D finite element model on the expectation that faulting and basalt intrusions are primarily sensitive to the magnitude and orientation of the least principal stress in extensional terranes. We found that in the absence of fault slip, variation in overburden pressure caused a stress state that preferentially favored intrusions at Crater Flat. However, when we allowed central Yucca Mountain faults to slip in the model, we found that magmatic clustering was not favored at Crater Flat or in the central Yucca Mountain block. Instead, we calculated that the stress field was most encouraging to intrusions near fault terminations, consistent with the location of the most recent volcanism at Yucca Mountain, the Lathrop Wells cone. We found this linked fault and magmatic system to be mutually reinforcing in the model in that dike inflation favored renewed fault slip.

INTRODUCTION

Yucca Mountain and its proposed high-level nuclear repository are embedded within crust deformed by normal faulting, plate-boundary shear, and basaltic volcanism (e.g., Morris et al., 2004 and references contained therein). The likelihood of tectonic events disrupting the repository site is of keen interest. Of particular concern is the possibility that the repository could be breached by renewed basaltic intrusion. Quantification of probable location and timing of future intrusions is guided by geologic information and expert knowledge (Crowe et al., 1982; Ho and Smith, 1997; Connor et al., 2000; Coleman et al., 2004). We attempt to supplement that knowledge by noting that orientation and location of basalt intrusions are controlled by the crustal stress field (e.g., Nakamura, 1977; Rubin and Pollard, 1988), and by using 3-D finite element methods to calculate regional crustal stresses. We include stresses imparted by regional extension, variable overburden pressure, and influences from oblique normal faulting. Additionally, we examine stresses imposed by magmatism back onto local faults.

Neotectonic Setting of Central Yucca Mountain

Yucca Mountain is a series of Miocene-aged volcanic tuffs sliced by north-south trending oblique normal faults; the most important (e.g. Morris et al., 2004; Potter et al., 2004) of these faults with late Quaternary activity are the Solitario Canyon (earthquakes occurred ~30 and 75 k.y.a.; Ramelli et al., 2004) Windy Wash (earthquakes occurred ~3, 40, and 75 k.y.a.; Whitney et al., 2004), and Fatigue Wash faults (earthquakes occurred ~9, 38, and 75 k.y.a.; Coe et al., 2004). The Yucca Mountain region has also been magmatically active since Miocene time. After cessation of the caldera-related tuff eruptions, small-volume basalt eruptions continued. Basalt volumes have declined steadily, but there are several ~1-m.y.-old cinder cones near Yucca Mountain (Sawyer et al., 1994; Crowe et al., 1995). The 0.08-m.y.-old Lathrop Wells cone resulted from the most recent intrusive event, about 15 km southwest of the proposed repository site. Several buried intrusions were identified with aeromagnetic techniques (e.g., O'Leary et al., 2002), mostly south of Yucca Mountain, and are of indeterminate age, save one that was drilled and dated at ~3.7 Ma.

There is paleoseismic evidence for temporal clustering of earthquakes and magmatism at Yucca Mountain. Abundant ash from the ~78.k.y.-old Lathrop Wells cone was found in earthquake fissures in trenches across the Solitario Canyon, Fatigue Wash, and Windy Wash faults (Keefer and Menges, 2004). It is likely that earthquakes occurred either during or very shortly after (weeks to months) the Lathrop Wells eruption because fissures typically begin to infill after the first significant rainfall (Ramelli et al., 2004).

MODELING

We simulated central Yucca Mountain crustal deformation using a 3-D finite element model. The model had cuts in it that corresponded with the dipping (~70°W; Menges and Whitney, 2004) Solitario Canyon, Fatigue Wash, and Windy Wash faults. Major corrugation features of the oblique-normal faults observed at the surface were assumed to extend to depth (Ferrill et al., 1999). The modeled crust was composed of 10-node elastic tetrahedral elements, while faults were lined with zero-thickness contact elements that obeyed Coulomb friction behavior (e.g., Parsons, 2002). The model simulated a 15-km-thick upper crust, the top of which was located 3 km below sea level. Model boundaries extended at least 50 km from the central Yucca Mountain region to avoid boundary conditions contaminating the solutions. All model elements were given uniform density of 2720 kg/m^3.

Model loads

Orientation and location of tabular basaltic intrusions of the type that feed cinder cones are sensitive to the magnitude and direction of the least principal stress (e.g., Nakamura, 1977; Rubin and Pollard, 1988). Thus all processes that influence crustal stress are also expected to influence magmatism. Our model included loading by four mechanisms: (1) variable pressure from the overburden, (2) remote regional extension, (3) slip on faults, and (4) opening of dikes.

A point at depth in the crust experiences pressure resulting from the weight of the overburden. The amount of pressure is a result of the integrated density of the rock above it, which varies with topography and lithology. A convenient way to calculate the overburden pressure is to use variations in the free air gravity anomaly (Δg_{fa}), which is sensitive to topography and crustal density. If we assume that Δg_{fa} can be approximated by a slab of thickness $h+t$, where h is a reference depth and t is elevation above sea level, then $\Delta g_{fa} = 2\pi\gamma\overline{\rho}(h+t)$, where $\overline{\rho}$ is mean density, and γ is Newton's gravitational constant. Pressure, (P) being the integrated density is given by

$$P = G\int_{0}^{h+t} \rho(z)dz, \tag{1}$$

where G is gravitational acceleration, and z is depth. Average density is then

$$\overline{\rho} = \frac{1}{h+t}\int_{0}^{h+t} \rho(z)dz. \tag{2}$$

Solving for pressure yields $P{=}G\Delta g_{fa}/2\pi\gamma$, which when the constants are expressed numerically, allows us to arrive at the simple result that $P{=}0.234\Delta g_{fa}$ in units of MPa. Accounting explicitly for topographic variations, rather than using the slab approximation, can be done but only makes very slight differences in the calculated pressure values.

The finite element model was loaded by pressure applied to its top (a depth of 3 km, which lies beneath the deepest parts of Crater Flat basin (Brocher et al., 1998)) according to variations in the free air gravity anomaly (Fig. 1). In addition to the variable pressure applied to the model top, it was allowed to compress under gravity, with the model base held fixed in the vertical dimension. Regional extension drives faulting and magmatism at Yucca Mountain with an observed least principal stress direction of ~N60°W (Stock et al., 1985; Harmsen, 1994; Morris et al., 1996). We therefore applied extensional displacements to the model edges at a rate of 20 nstrain yr^{-1} on a N60°W orientation, consistent with geodetic (Savage et al., 2001) and geologic (Fridrich et al., 1999) rates.

We ran a progression of tests to examine different influences on the 3D stress field at Yucca Mountain. Initially, we applied only overburden pressure and gravity loading to isolate their effects in the absence of remote extension. Next, since the major central Yucca Mountain faults predate the Lathrop Wells cone, we extended the model for a calculated 80 k.y. period (time since last eruption and simulates ~2 seismic cycles), allowed the faults to slip freely, and examined stress changes. Lastly, we calculated stress changes caused by inflation of our estimated most-likely Lathrop Wells feeder dike.

Model Results

Given that basaltic intrusions are encouraged under extension where the least principal stress is lowest magnitude, we tested a hypothesis that suggests in the absence of other influences, intrusions might cluster preferentially where the overburden pressure is smallest. The results of this test indicated that influence from variation in overburden stress is not dominant in controlling where basalt intrudes the shallow crust (Fig. 1); the chain of ~1-m.y.-old cinder cones at Crater Flat are located at a calculated low least-principal-stress zone, whereas Lathrop Wells and a series of buried basalt intrusions correspond with higher calculated least principal stress. We included overburden pressure as a contributing effect in subsequent calculations.

Normal faulting and basaltic intrusions are observed to accommodate tectonic extension interchangeably since both processes cause strain and increase the least principal stress (Parsons and Thompson, 1991). We sought to calculate crustal stresses resulting from the combination of remotely applied extension and slip on faults. Major central Yucca Mountain faults significantly predate the Lathrop Wells cone (Potter et al., 2004), so we allowed the model faults to slip freely under applied extension for a simulated 80 k.y. period. The duration of the simulation was chosen to be long enough to represent multiple earthquakes on each fault (Keefer and Menges, 2004), and to coincide with the time elapsed since the last volcanic eruption. In the model, the faults accumulated up to 2 m of slip (Fig. 2A) with highest slip rates on the Windy Wash fault, commensurate with observations (Fridrich et al., 1999). Mapping the calculated change in least principal stress resulting from fault slip shows the region around the faults to be less favorable to magmatic intrusion, whereas regions north and south of the faults are more favorable, including the Lathrop Wells site (Fig. 2B). While the ~1-m.y.-old chain of cinder cones in Crater Flat was encouraged in the model when just overburden pressures were considered (Fig. 1), they would not be encouraged after slip on central Yucca Mountain faults (Fig. 2B).

To study the effects of dike intrusion on faults, we assumed that a vertical Lathrop Wells feeder dike(s) was oriented orthogonally (N30°E) to the least principal stress direction. We calculated that magma ascent would be most favored on the N30°E-striking plane at, and southwest of, the Lathrop Wells cone (Fig. 2C). To calculate stress-change effects on central Yucca Mountain faults from a scenario Lathrop-Wells intrusion, we assumed a 2-m dike opening on the N30°E plane where the least principal stress was reduced by modeled fault slip (blue areas on Fig. 2C). We found that such an intrusion would have increased Coulomb failure stress (increasing likelihood of slip) on all three major faults in the model, with the strongest effect on the Solitario Canyon and Fatigue Wash faults (Fig. 3).

We calculated that the Lathrop Wells intrusion decreased the least principal stress north of the modeled dike in the Yucca Mountain block. In Figure 3 we show this as increased likelihood of normal-fault slip. That same stress change would encourage more dike intrusion to the north as well. Evidence from the paleoseismic record indicates that instead of more intrusions into the Yucca Mountain block, each of the major faults had at least 1-2 earthquakes subsequent to the Lathrop Wells eruption (Keefer and Menges, 2004).

CONCLUSIONS

Observation of volcanic ash in the bottoms of fissures along major Yucca Mountain faults demonstrates temporal clustering of earthquakes and a volcanic eruption. We found using a 3D finite element model that slip on faults and dike opening can work in concert to accommodate extension at Yucca Mountain. The inferred geometry of the system appears to mutually enhance both processes. We found in the absence of fault slip, that overburden pressure creates a stress state favoring clustering of magmatic intrusions at Crater Flat (Fig. 1). However, we also found that after fault slip, volcanic clustering is less likely in the Crater Flat region, and is instead favored near terminations of the major faults (Fig. 2B). Given that the central Yucca Mountain faults have all slipped at least twice since the last volcanic episode, we conclude that the stress field favors basalt intrusions near and southwest of the Lathrop Wells site, and north of the major faults in the Claim Canyon Caldera region (Fig. 2B).

REFERENCES CITED

Brocher, T. M., Hunter, W. C., and Langenheim, V. E., 1998, Implications of seismic reflection and potential field geophysical data on the structural framework of the Yucca Mountain-Crater Flat region, Nevada: Geological Society of America Bulletin, v. 110, p. 947-971.

Coe, J. A., Oswald, J., Vadurro, G., and Lundstrom, S. C., 2004, Quaternary Faulting on the Fatigue Wash Fault, *in* Keefer, W. R., Whitney, J. W., and Taylor, E. M., eds., Quaternary Paleoseismology and Stratigraphy of the Yucca Mountain Area, Nevada: U. S. Geological Survey Professional Paper 1689, p. 111-124.

Coleman, N. M., Abramson, L. R., and Marsh, B. D., 2004, Testing claims about volcanic disruption of a potential geologic repository at Yucca Mountain, Nevada: Geophysical Research Letters, v. 31., doi:10.1029/2004GL021032.

Connor, C. B., Stamatakos, J. A., Ferrill, D. A., Hill, B. E., Ofoegbu, G. I., Conway, F. M., Sagar, B., and Trapp, J., 2000, Geologic factors controlling patterns of small-volume basaltic volcanism: application to a volcanic hazards assessment at Yucca Mountain, Nevada: Journal of Geophysical Research, v. 105, p. 415-432.

Crowe, B. M., Perry, F. V., Geissman, J., McFadden, L. D., Wells, S. G., Murrell, M., Poths, J., Valentine, G. A., Bowker, L., and Finnegan, K., 1995, Status of volcanism studies for the Yucca Mountain site characterization project: Los Alamos, New Mexico, Los Alamos National Laboratory Report LA-12908-MS, 363 pp.

Ferrill, D. A., Stamtakos, J. A., and Sims, D., 1999, Normal fault corrugation: implications for growth and seismicity of active normal faultsL Journal of Structural Geology, v. 21, p. 1027-1038.

Fridrich, C. J., Whitney, J. W., Hudson, M. R., and Crowe, B. M., 1999, Space-time patterns of late Cenozoic extension, vertical axis rotation and volcanism in the Crater Flat basin, southwest Nevada, *in* Wright, L. A., and Troxel, B. E., eds., Cenozoic Basins of the Death Valley Region: Boulder, Colorado, Geological Society of America Special Paper, v. 333, p. 197-212.

Harmsen, S. C., 1994, The Little Skull Mountain, Nevada, earthquake of 29 June 1992: aftershock focal mechanisms and tectonic stress field implications: Bulletin of the Seismological Society of America, v. 84, p. 1484-1505.

Ho, C-H, and Smith, E. I., 1997, Volcanic hazard assessment incorporating expert knowledge: application to the Yucca Mountain region, Nevada, USA: Mathematical Geology, v. 29, p. 615-627.

Keefer, W. R., and Menges, C. M., 2004, Summary of the temporal and spatial relations of Quaternary faulting during the past 100 k.y. at Yucca Mountain: Evidence for distributive surface ruptures on multiple faults, *in* Keefer, W. R., Whitney, J. W., and Taylor, E. M., eds., Quaternary Paleoseismology and Stratigraphy of the Yucca Mountain Area, Nevada: U. S. Geological Survey Professional Paper 1689, p. 197-200.

Menges, C. M., and Whitney, J. W., 2004, Distribution of Quaternary faults at Yucca Mountain, *in* Keefer, W. R., Whitney, J. W., and Taylor, E. M., eds., Quaternary Paleoseismology and Stratigraphy of the Yucca Mountain Area, Nevada: U. S. Geological Survey Professional Paper 1689, p. 23-31.

Morris, A. P., Ferrill, D. A., and Henderson, D. B., 1996, Slip tendency analysis and fault reactivation: Geology, v. 24, p. 275-278.

Morris, A. P., Ferrill, D. A., Sims, D. W., Franklin, N., and Waiting, D. J., 2004, Patterns of fault displacement and strain at Yucca Mountain, Nevada: Journal of Structural Geology, v. 26, p. 1707-1725.

Nakamura, K., 1977, Volcanoes as possible stress indicators of tectonic stress orientation - principle and proposal: Journal of Volcanology and Geothermal Research, v. 2, p. 1-16.

O'Leary, D. W., Mankinen, E. A., Blakely, R. J., Langenheim, V. E., and Ponce, D. A., 2002, Aeromagnetic expression of buried basaltic volcanoes near Yucca Mountain, U. S. Geological Survey Open File Report 02-020, 52 pp.

Parsons, T., 2002, Post-1906 stress recovery of the San Andreas fault system from 3-D finite element analysis, Journal of Geophysical Research, v. 107, 2162, doi:10.1029/2001JB001051.

Parsons, T., and Thompson, G. A., 1991, The role of magma overpressure in suppressing earthquakes and topography: Worldwide examples: Science, v. 253, p. 1399-1402.

Potter, C. J., Day, W. C., Sweetkind, D. S., and Dickerson, R. P., 2004, Structural geology of the proposed site area for a high-level radioactive waste repository, Yucca Mountain, Nevada: Geological Society of America Bulletin, v. 116, p. 858-879.

Ramelli, A. R., Oswald, J. A., Vadurro, G., Menges, C. M., and Paces, J. B., 2004, Quaternary Faulting on the Solitario Canyon Fault, *in* Keefer, W. R., Whitney, J. W., and Taylor, E. M., eds., Quaternary Paleoseismology and Stratigraphy of the Yucca Mountain Area, Nevada: U. S. Geological Survey Professional Paper 1689, p. 89-109.

Rubin, A. M., and Pollard, D. D., 1988, Dike-induced faulting in rift zones of Iceland and Afar: Geology, v. 16, p. 413-417.

Savage, J. C., Svarc, J. L., and Prescott, W. H., 2001, Strain accumulation near Yucca Mountain, Nevada, 1993-1998, Journal of Geophysical Research, v. 106, p. 16483-16488.

Sawyer, D. A., Fleck, R. J., Lanphere, M. A., Warren, R. G., Broxton, D. E., and Hudson, M. R., 1994, Episodic caldera volcanism in the Miocene southwest Nevada volcanic field: revised stratigraphic framework, $^{40}Ar/^{39}Ar$ geochronologic framework, and implications for magmatism and extension: Geological Society of America Bulletin, v. 106, p. 1304-1318.

Stock, J. M., Healy, J. H., Hickman, S. H., and Zoback, M. D., 1985, Hydraulic fracturing stress measurements at Yucca Mountain, Nevada, and relationship to regional stress field: Journal of Geophysical Research, v. 90, p. 8691-8706.

Whitney, J. W., Simonds, F. W., Shroba, R. R., and Murray, M., 2004, Quaternary Faulting on the Windy Wash Fault, *in* Keefer, W. R., Whitney, J. W., and Taylor, E. M., eds., Quaternary Paleoseismology and Stratigraphy of the Yucca Mountain Area, Nevada: U. S. Geological Survey Professional Paper 1689, p. 125-134.

FIGURE CAPTIONS

Figure 1. (A) Vertical pressure at 3 km depth exerted by the overburden as calculated from the free air gravity anomaly (see text for derivation). Pressures tend to be higher where topography and/or shallow crustal density is highest. Cross section A-A' in (B) shows an example relationship between topography and the free air anomaly; this section corresponds with the seismic model of Brocher et al. (1998). (C) Calculated least principal stress magnitudes in an unbroken elastic slab averaged over 3-6 km depth resulting from the applied pressures shown in (A). Lower values (blue colors) are places where basalt intrusions might be more favored in the absence of other stress influences.

Figure 2. (A) Modeled central Yucca Mountain faults contoured with 80 k.y. of slip caused by remote extension. Negative slip implies a rake change caused by basal model boundary conditions. (B) Mapped change in least principal stress magnitude resulting from the fault slip shown in (A). Warm colors (least stress

increased) indicate areas less favored for basalt intrusions, while cool colors indicate places where fault slip encourages intrusion. Contour scale is the same as in (C), where the magnitude of the least principal stress is projected onto a N30°E striking plane, which is orthogonal to the extension direction and thus a likely orientation for basalt feeder dikes at Lathrop Wells.

Figure 3. Coulomb stress change on the Solitario Canyon, Fatigure Wash, and Windy Wash faults from a scenario dike opening beneath Lathrop Wells. We modeled a 2-m opening on the N30°E-striking plane shown in map view at locations where the least stress was reduced by fault slip as shown in Fig. 2C. In this scenario, fault slip and dike opening are mutually reinforcing processes.

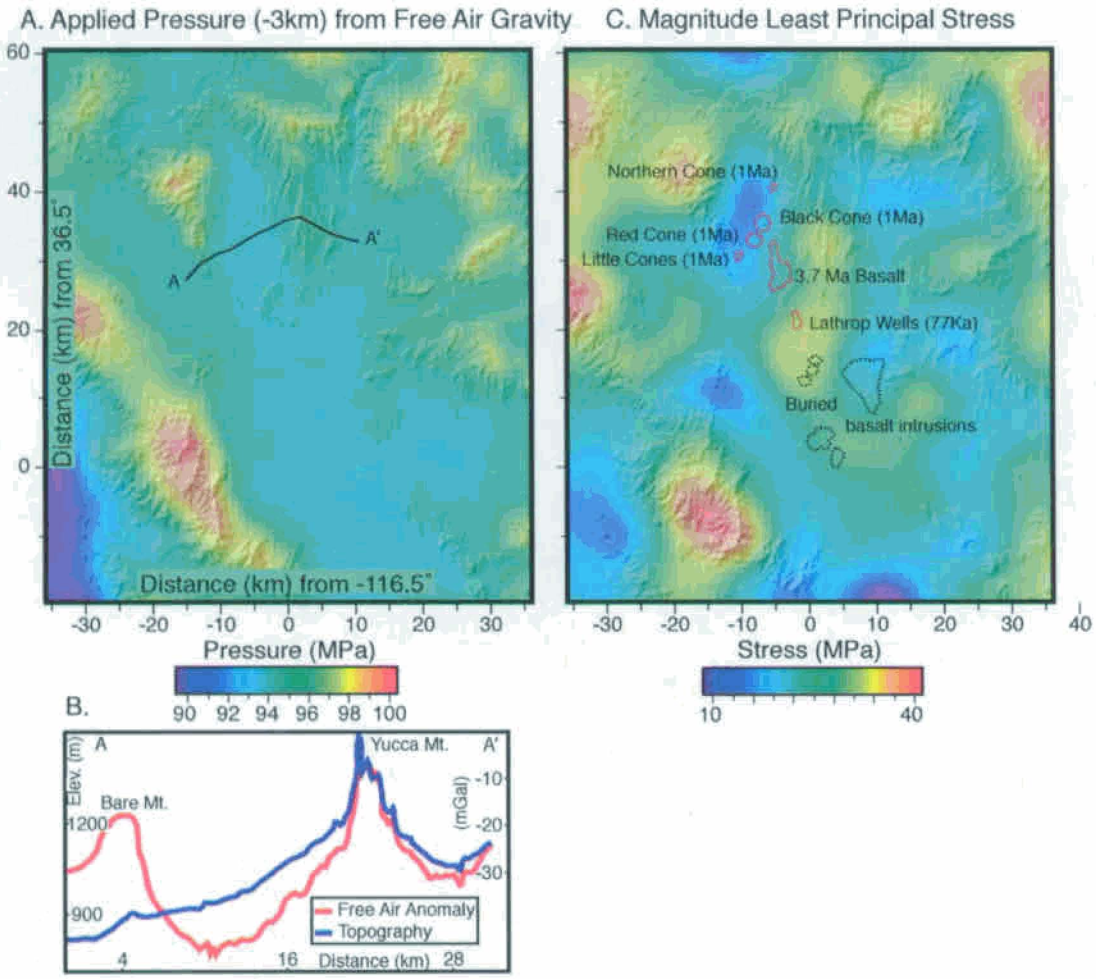

A. Applied Pressure (-3km) from Free Air Gravity
C. Magnitude Least Principal Stress
Distance (km) from 36.5°
Distance (km) from -116.5°
A
A'
Northern Cone (1Ma)
Black Cone (1Ma)
Red Cone (1Ma)
Little Cones (1Ma)
3.7 Ma Basalt
Lathrop Wells (77Ka)
Buried
basalt intrusions
Pressure (MPa)
90 92 94 96 98 100
Stress (MPa)
10
40
B.
Elev. (m)
Bare Mt.
Yucca Mt.
(mGal)
Free Air Anomaly
Topography
Distance (km)

Figure 1

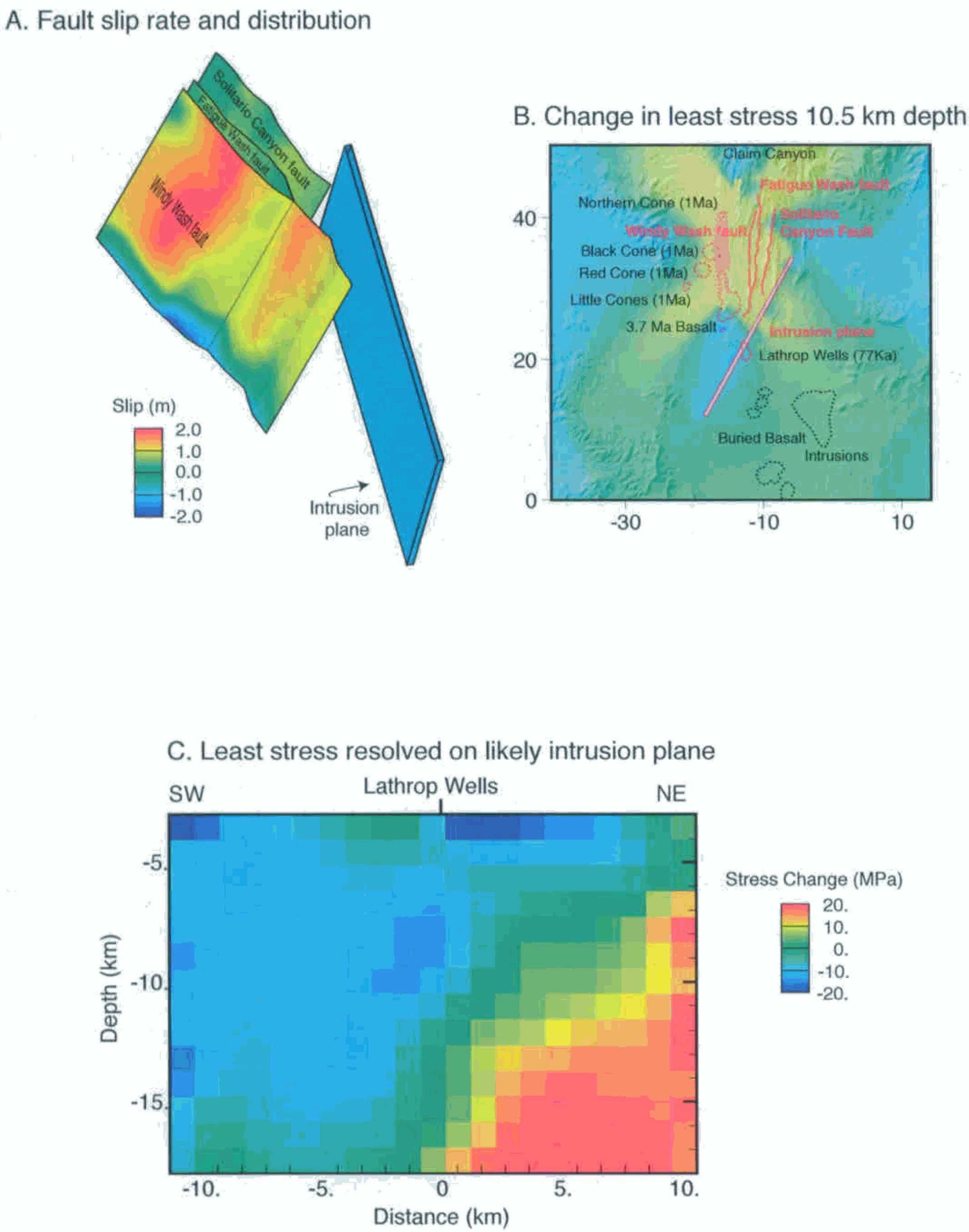
A. Fault slip rate and distribution
Solitario Canyon fault
Fatigue Wash fault
Windy Wash fault
Slip (m)
2.0
1.0
0.0
-1.0
-2.0
Intrusion plane
B. Change in least stress 10.5 km depth
Claim Canyon
Fatigue Wash fault
Northern Cone (1Ma)
Windy Wash fault
Solitario Canyon Fault
Black Cone (1Ma)
Red Cone (1Ma)
Little Cones (1Ma)
3.7 Ma Basalt
Intrusion plane
Lathrop Wells (77Ka)
Buried Basalt
Intrusions
40
20
0
-30
-10
10
C. Least stress resolved on likely intrusion plane
SW
Lathrop Wells
NE
Depth (km)
-5.
-10.
-15.
-10.
-5.
0
5.
10.
Distance (km)
Stress Change (MPa)
20.
10.
0.
-10.
-20.

Figure 2

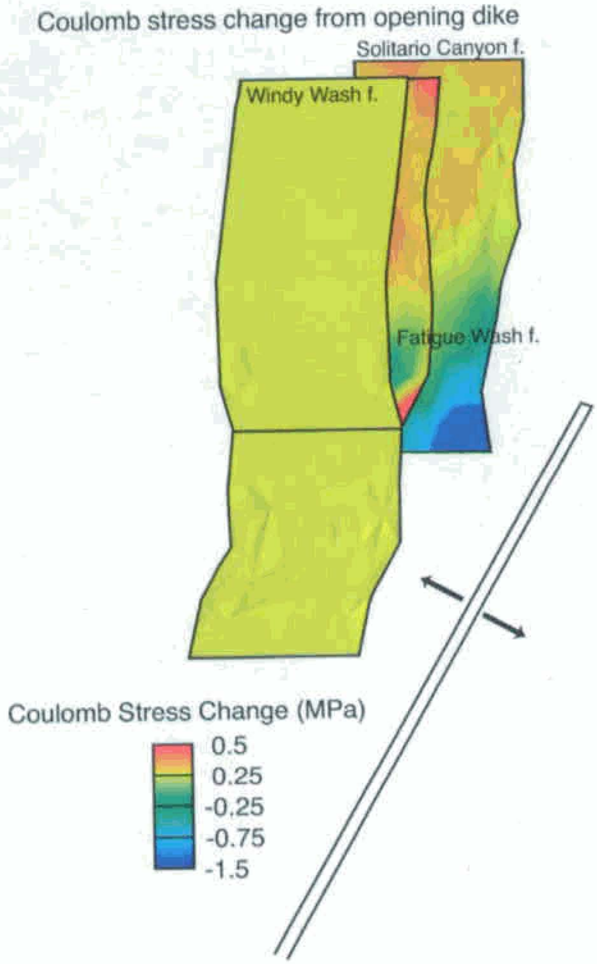

Coulomb stress change from opening dike
Solitario Canyon f.
Windy Wash f.
Fatigue Wash f.
Coulomb Stress Change (MPa)
0.5
0.25
-0.25
-0.75
-1.5

Figure 3